Shock Waves (2002) 12: 69–78
Digital Object Identifier (DOI) 10.1007/s00193-002-0136-3

Shock Waves

Size of craters produced by explosive charges on or above the ground surface

R.D. Ambrosini[1], B.M. Luccioni[1], R. F. Danesi[1], J.D. Riera[2], M.M. Rocha[2]

[1] Instituto de Estructuras, Universidad Nacional de Tucumán, CONICET, Argentina
[2] CPGEC, Univ. Federal de Rio Grande do Sul, Porto Alegre, CNPq, Brasil

Received 19 April 2000 / Accepted 12 December 2001
Published online 11 June 2002 –

Abstract. The results of a series of tests performed with different amounts of explosive at short distances above and below ground level, as well as on the soil surface are briefly described. After an introductory description of both the main features of the blast wave and the mechanics of crater formation, a brief review of empirical methods for crater size prediction is presented. Next, the experimental design and the results obtained are described. The crater dimensions for underground explosions coincide with those found in the literature. For explosions at ground level the results are qualitatively described by empirical equations. For explosive charges situated above ground level, the dimensions of the craters are smaller than those observed in underground and near the surface explosions. Two new single prediction equations for this case are presented.

Key words: Blast loading, Craters, Soil

1 Introduction

Blasting loads have come into attention in recent years due to the great number of accidental or intentional events that affected important structures all over the world, clearly indicating that the issue is relevant for purposes of structural design and reliability analysis. In consequence, extensive research activities in the field of blast loads have taken place in the last few decades.

Dynamic loads due to explosions result in strain rates of the order of 10^{-1} to 10^{3} s^{-1} which imply short time dynamic behavior of the materials involved, characterized mainly by a great overstrength and increased stiffness, in comparison with normal, static properties. In the case of soils, the response and the mechanism of crater formation are still more complex due to the usual anisotropy and non linear nature of the material, to the variability of mechanical properties and the coexistence of the three phases: solid, liquid and gaseous. Generally, simplifying assumptions must be made in order to solve specific problems. Until now, most practical problems have been solved through empirical approaches. Years of industrial and military experience have been condensed in charts or equations (Baker et al. 1983; Smith and Hetherington 1994). These are useful tools, for example, to establish the weight of explosive to yield a perforation of certain dimensions or to estimate the type and amount of explosive used in a terrorist attack, from the damage registered. Most research is related to underground explosions and only a few papers are concerned with explosions at ground level. Studies about craters produced by explosions above ground level, which would be the case when the explosive charge is situated in a vehicle, are rarely found in the open technical literature. Some reports are classified information limited to government agencies.

Correspondence to: R.D. Ambrosini
(e-mail: dambrosini@herrera.unt.edu.ar)

2 Blast waves

When a condensed high explosive is detonated a blast wave is formed. A typical pressure-time profile for a blast wave in free air is shown in Fig. 1. It is characterized by an abrupt pressure increase at the shock front, followed by a quasi exponential decay back to ambient pressure p_o and a negative phase in which the pressure is less than ambient. Of particular importance are the following wavefront parameters:

p_s : peak overpressure
T_s : duration of the positive phase
i_s : specific impulse of the wave which is the area beneath the pressure-time curve from the arrival at time t_a to the end of the positive phase.

The pressure-time history of a blast wave is often described by exponential functions such as Frielander's equa-

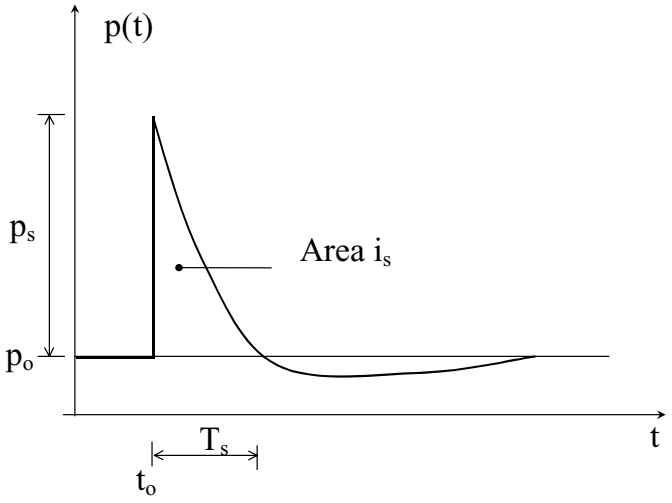

Fig. 1. Blast wave pressure-time history

tion (Smith and Hetherington 1994), which has the form

$$p(t) = p_s \left[1 - \frac{t}{T_s}\right] \exp\left\{-\frac{bt}{T_s}\right\} \qquad (1)$$

where b is a positive constant called the waveform parameter that depends on the peak overpressure p_s. The most widely used approach to blast wave scaling is Hopkinson's law (Baker et al. 1983) which establishes that similar explosive waves are produced at identical scaled distances when two different charges of the same explosive and with the same geometry are detonated in the same atmosphere. Thus, any distance R from an explosive charge W can be transformed into a characteristic scaled distance Z

$$Z = \frac{R}{W^{1/3}} \, . \qquad (2)$$

The use of Z allows a compact and efficient representation of blast wave data for a wide range of situations. In expression (2), W is the charge mass expressed in kilograms of TNT. To quantify blast waves from sources other than TNT, the actual mass of the charge must be converted into an equivalent TNT mass. This is achieved by multiplying the mass of explosive by a conversion factor based on the specific energy, the peak overpressure or the impulse delivered (Baker et al. 1983).

3 Crater formation: brief state of the art

Tests of crater formation are appropriate tools to study the blast phenomena, the behavior and destructive power of different explosives and the response of soils and rocks under this type of load (Persson et al. 1994). The mechanism of crater formation is complex and is related to the dynamic physical properties of air, soil and soil-air interface. Even very carefully performed cratering tests give deviations in the dimensions measured of the order of 10%, while differences of as much as 30% to 40% are common (Bull and Woodford 1998).

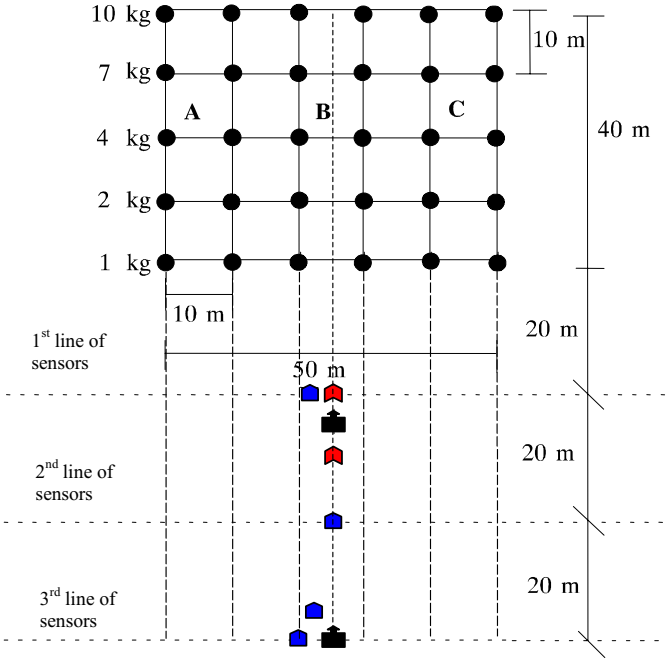

References

Acceleration transducers

Pressure transducers

Data acquisition equipment

A= 2 Series at ground level

B = 2 Series at 50 cm over the ground level

C = A serie a at 1m over the ground level and serie b at 1m underground

Fig. 2. Loads and measurement equipment locations

A cavity is always formed when a confined explosion is produced in a mass of soil. If the explosion is close to the surface, a crater is formed, a complex interaction taking place between gravity effects, soil strength and transient load conditions. The most important variables in defining the crater shape and size are the mass W of the explosive and the depth of the detonation beneath the air/soil interface d. When $d < 0$, the explosive is detonated over the air/soil interface, $d = 0$ when the detonation occurs in the air/soil interface and $d > 0$ when the explosive is detonated beneath the soil surface. For $d > 0$, the crater mechanism is altered by gravitational effects. When the depth of the detonation increases, larger amounts of subsoil must be expelled by the explosion. Thus the crater radius and the depth of the crater increase when d increases, until a certain limit value, from which they rapidly decrease (Bull and Woodford 1998).

Studies concerned with the characteristics of craters caused by explosions usually resort to dimensional analysis and statistics. The scaling law establishes that any linear dimension "L" of the crater can be expressed as a constant multiplied by W^{α} divided by the distance of the charge from the ground, where W represents the equivalent TNT mass of explosive and α is a coefficient depending upon if gravitational effects can be neglected or not. In the first case the cubic root law is applicable ($\alpha = 0.33$) and in

the other cases the functional dependence can be quite complex.

Baker et al. (1991) presents a dimensional study to model the crater formation phenomenon in the case of underground explosions. Six parameters are chosen to define the problem: the explosive mass W, the depth of the explosive charge d, the apparent crater radius R, the soil density ρ, and two strength parameters to define the soil properties: one with the dimensions of a stress σ, related to soil strength, and the other with the dimensions of a force divided by a cubic length (Nm^{-3}) K, that takes into account gravitational effects.

After a dimensional analysis and many empirical observations, the following functional relation may be obtained (Baker et al. 1991)

$$\frac{R}{d} = f\left(\frac{W^{7/24}}{\sigma^{1/6}K^{1/8}d}\right) . \tag{3}$$

If $\frac{R}{d}$ (scaled radius of the crater) is plotted as a function of $W^{7/24}/d$, it can be seen that this relation is close to experimental results and can be approximately simplified by two straight lines, one with a moderate slope for $W^{7/24}/d > 0.3$ and one steeper for $W^{7/24}/d < 0.3$. For $W^{7/24}/d < 0.3$, the scaled radius of the crater is sensible to small changes in the independent parameter and, due to this fact, the dependent parameter or the scaled radius may exhibit great variability. Experimental conditions are better controlled for $W^{7/24}/d > 0.3$.

It can be deduced that the specific weight ρg is the best measure for$K$and that ρc^2 is the best measure for σ, where c is the seismic velocity in the soil. If experimental results for different types of soils are plotted in a $\frac{R}{d}$ versus $\frac{W^{7/24}}{\rho^{7/24}c^{1/3}g^{1/8}d}$ graph, it may be clearly seen that there is very little variability in the results.

The preceding paragraph refers to underground explosions. There is less information about explosions at ground level. Statistical studies of about 200 accidental aboveground explosions of relative large magnitude are presented by Kinney and Graham (1985). The results exhibit a variation coefficient of about 30%. From these results, the following empirical equation for the crater diameter is proposed

$$D\ [m] = 0.8W[Kg]^{1/3} . \tag{4}$$

Additional experimental evidence was obtained during the surface explosions performed by EMRTC (Energetic Materials Research Center of the Mineralogical and Technologic Institute of New Mexico). EMRTC conducted experimental determinations to explore alternative ways of controlling the blasting power. In this program, a 3.8 m diameter crater was formed by the explosion of 250 kg of TNT situated at ground level.

In connection with the morphological and structural types of the craters, Jones et al. (1997) present an extensive study of high explosion and planetary impact craters and determine three different basic types: (a) bowl-shaped, (b) flat-floored with central uplift and (c) flat floored with multirings. One of the factors that determines the shape is the height of burst. On the other hand, numerical and independent research results presented by Iturrioz et al. (2001) preliminary confirm the formation of the same shapes of craters.

Additionally, Gorodilov and Sukhotin (1996) present the results of research about the shape and size of craters generated by explosions of underwater surface charges on sand.

The depth of the crater created by an explosion ordinarily is about one quarter its diameter, but this depends on the type of soil involved (Kinney and Graham 1985).

4 Tests description

In order to study blast phenomena and its effects on soils, three sets of tests have been performed.

4.1 Site location and soil mechanical properties

The tests were performed in a large flat region, without rock formations, normally used for agriculture. Two exploratory drillings and two test pits were used to determine the mechanical properties of the soil. The exploratory holes were drilled to depths of 2 m and 5 m, respectively, with standard penetration tests (SPT) performed at 1m intervals. The test pits were dug to a depth of 2 m in order to collect undisturbed soil samples for triaxial testing and for a more precise determination of the *in situ* density.

The results of the tests are presented in Tables 1 to 4. The soil profile was quite uniform in the entire 40×50 m testing area, being characterized by

1) 0 to 0.70 m	Brown clayey silt with organic matter.
2) 0.70 to 5.0 m	Reddish brown clayey silt of low plasticity, classification CL, very dry.

4.2 Test series

The tests were performed in a selected 40 m × 50 m area. A grid with a 10m spacing was used to locate the explosive charges at its nodes, as shown in Fig. 2. Each row of the grid corresponded to loads of the same magnitude. Charges equivalent to 1, 2, 4, 7 and 10 kg of TNT were located on the five rows. All the charges were spherical. In the first two columns indicated as "A" in Fig. 2, the explosives were situated tangential to the surface. In the following columns designated as "B" in Fig. 2, the explosives were located 0.5 m above ground level. Finally, in the last two columns indicated as C1 and C2 in Fig. 2, the loads were situated 1 m above ground level (Fig. 3) and 1 m underground respectively. The charges above ground level were located hanging on wood tripods (Fig. 3).

Fig. 3. Elevated-charge support system

a

b

Fig. 4a,b. Blasting tests. **a** Ground level explosion; **b** underground explosion

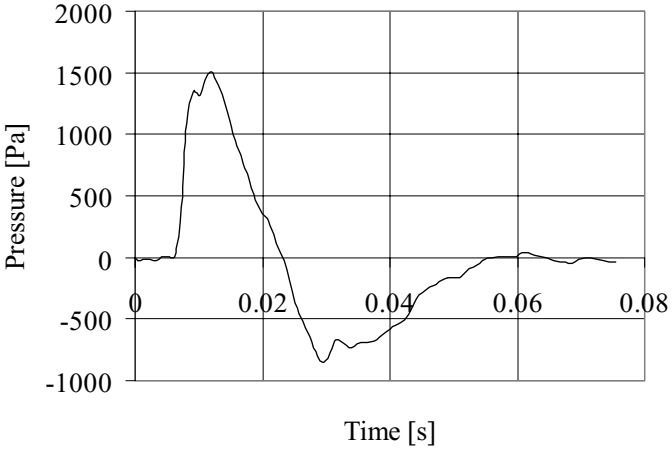

Fig. 5. Recorded blast wave pressure-time history

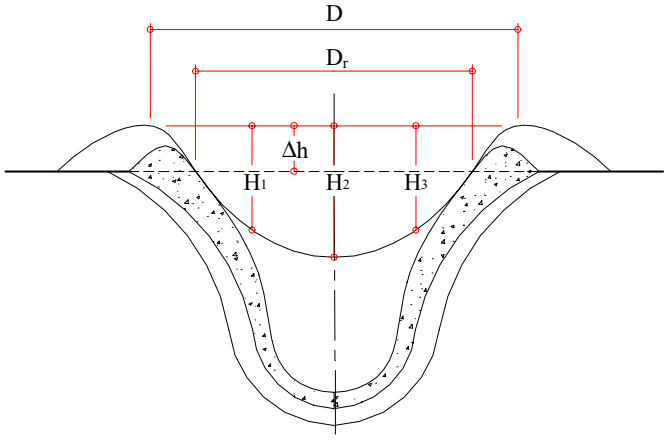

Fig. 6. Definitions of the crater dimensions

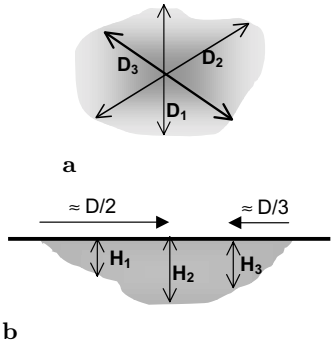

Fig. 7a,b. Crater measurements. **a** Diameter measurements. **b** Depth measurements

4.3 Explosive description

The explosive used in the tests was Gelamón 80, a NG based gelatinous explosive theoretically equivalent in mass to 80% TNT. This explosive is similar to Special Gelatine 80 (Formby and Wharton 1996). The weights of explosive used in each test are indicated in Table 5.

4.4 Measurement settings

The measurement equipment was basically composed of:

a) Acceleration transducers type AS-10TB and AS-5GB, by Kyowa, to measure soil accelerations. The signals from the transducers were amplified by a Kyowa signal conditioning system DPM-612B, calibrated for 1000 and 2000 mV/g, low-pass filtered at 300 Hz
b) Differential pressure transducers type 163PC, by Honeywell, to measure overpressures in air. These transducers are internally pre-amplified. The calibration constant for operation with a regulated 8 V power source is around 2 mV/Pa, with peak capability of 1500 Pa. The excessive sensibility for this application prevented the transducers to be closer than 40 m of the blast source, due to possible saturation. The transducer dynamic response had been previously tested up to 200 Hz, which is recognizably only a fraction of the acquisition rate.

All signals have been AD converted by a data acquisition system consisting of a notebook with a sixteen channel PCMCIA Card type DAS 16/330 by Computerboards. The acquisition rate was set to 1024 Hz.

5 Tests results

Figure 4 show two blasting tests corresponding to a detonation at ground level and an underground explosion.

5.1 Pressure measurements

Pressure-time recordings were obtained from pressure transducers. Many of them do not exhibit a typical blast wave characteristic as that represented in Fig. 1. They appear to involve superposition of different blast waves and noise. An example of a recorded blast wave is presented in Fig. 5. It corresponds to test B7b. Limitations of the measurement system, discussed in the previous section, render the recorded pressures useful for descriptive or qualitative purposes only.

5.2 Crater size measurements

The following comments apply to the crater size measurement procedure:

(a) The *apparent* crater diameter D (Fig. 6) was measured in all cases according to the definition given by Kinney and Graham (1985)
(b) 3 measurements of the crater diameter and 3 of the crater depth were performed, according to Fig. 7.
(c) In general, the craters produced by explosives situated at ground level presented a small mound in the center formed by the loose soil that fell down on the site after the explosion. This mound was removed to measure height H_2 (Fig. 6).

Table 1. Soil properties – Drilling S-1

Depth [m]	Phreatic Level	Type of soil	SPT tests		HD t/m^3	DD t/m^3	H	T200	LL %	PI %	Clas./ UCS
			Depth [m]	N							
0.7		(1)	0.5-1.0	6	1.25	1.14	9.6	87	28.1	12.3	CL
1.0			1.5-2.0	12	1.43	1.27	12.7	91	27.9	8.6	CL
2.0	without										
3.0	phreatic	(2)					19.3	95	31.0	10.4	CL
4.0	water										
5.0			End of the drilling								

HD: Humid density; DD: Dry density; H: Humidity; T200: Percentage that passes through sieve N°200; LL: Liquid limit; PI: Plastic index; Clas. /UCS: Classification according UCS

Table 2. Soil properties – Drilling S-2

Depth [m]	Phreatic level	Type of soil	SPT Test		HD [t/m^3]	DD [t/m^3]	H	T200	LL %	PI %	CLAS. /UCS
			Depth [m]	N							
0.70	without phreatic water	(1)	0.5–1.0	9	1.33	1.22	9.2	88	28.1	10.7	CL
1.0		(2)	1.5–2.0	11	1.52	1.35	12.6	93	25.9	7.0	CL
2.0			End of the drilling								

HD: Humid density; DD: Dry density; H: Humidity; T200: Percentage that passes through sieve N°200; LL: Liquid limit; PI: Plastic index; Clas./UCS: Classification according UCS

Table 3. Soil properties – Trial pit C-1

Depth [m]	Phreatic level	Type of soil	Fric. (°)	Coh [MPa]	HD [t/m^3]	DD [t/m^3]	H	T200	LL %	PI %	Clas./ UCS
0.7	without	(1)									
1.0	phreatic	(2)	24	0.036	1.47	1.32	11.7				CL
2.0	water				1.61	1.45	11.2				CL

Fric.: Angle of internal friction; Coh.: Cohesion; HD: Humid density; DD: Dry density; H: Humidity; T200: Percentage that passes through sieve N°200; LL: Liquid limit; PI: Plastic index; Clas./UCS: Classification according UCS

Table 4. Soil properties – Trial pit C-2

Depth [m]	Phreatic level	Type of soil	Fric. (°)	Coh [MPa]	HD [t/m^3]	DD [t/m^3]	H	T200	LL %	PI %	Clas./ UCS
0.7	without	(1)									
1.0	phreatic	(2)			1.46	1.33	10.2				CL
2.0	water		25	0.026	1.64	1.43	14.7				CL-ML

Fric.: Angle of internal friction; Coh.: Cohesion; HD: Humid density; DD: Dry density; H: Humidity; T200: Percentage that passes through sieve N°200; LL: Liquid limit; PI: Plastic index; Clas./UCS: Classification according UCS

a

b

Fig. 8a,b. Craters obtained in two tests. **a** Superficial explosion crater; **b** underground explosion crater

(d) The shape of most of the craters was flat-floored with central uplift.

As illustration, the craters due to surface and underground explosions are shown in Fig. 8

The mean dimensions of the craters are indicated in Tables 6 to 9 for explosions at ground level, over the ground and underground, respectively.

6 Results analysis

6.1 Underground explosions

Due to the great number of published test results concerning underground explosions, these results are useful in order to verify that the mechanics of the process of the explosions were properly developed and to give an idea about the completeness of the detonations for small charges.

In Fig. 9 the results shown in Table 9 are presented graphically in conjunction with the experimental results presented by Baker et al. (1991) for alluvium soils. It can be seen in Fig. 9 that there is excellent agreement between the present results and the corresponding to Baker et al. (1991) although the types of soils involved are different. Moreover, for this case, the exponent $\alpha = 7/24$ is the most appropriate.

6.2 Explosions at ground level

In Fig. 10, the results corresponding to charges at ground level (Table 6) are presented in conjunction with straight lines defined by equation $4 \pm 30\%$. It can be seen that most of the values are between the mean and the -30%

Table 5. Mass of Gelamon 80 and theoretical equivalent TNT mass

Test	Mass of Gelamon 80 (kg)	Equivalent TNT mass (kg)
A1a	1.25	1
A1b	1.25	1
A2a	2.5	2
A2b	2.5	2
A4a	5.0	4
A4b	5.0	4
A7a	8.75	7
A7b	8.75	7
A10a	12.5	10
A10b	12.5	10
B1a	1.25	1
B1b	1.25	1
B2a	2.5	2
B2b	2.5	2
B4a	5.0	4
B4b	5.0	4
B7a	8.75	7
B7b	8.75	7
B10a	12.5	10
B10b	12.5	10
C1a	1.25	1
C1b	1.25	1
C2a	2.5	2
C2b	2.5	2
C4a	5.0	4
C4b	5.0	4
C7a	8.75	7
C7b	8.75	7
C10a	12.5	10
C10b	12.5	10

Table 6. Dimensions of the craters produced by explosions at ground level

Test	Mean diameter (cm)	Central depth (cm)	D/H_2 ratio
A1a	62	11	5.6
A1b	54	10.5	5.1
A2a	78	12.5	6.2
A2	70	12	5.8
A4a	95	17	5.6
A4b	73	21	3.5
A7a	158	21	7.5
A7b	138	22	6.3
A10a	148	22	6.7
A10b	164	31.5	5.2

Table 7. Dimensions of the craters produced by explosions located at 0.5 m above ground level

Test	Mean diameter (cm)	Central depth (cm)	D/H_2 h ratio
B1a	43	5	8.6
B1b	34	4.5	7.6
B2a	48	6.5	7.4
B2b	62	6.5	9.5
B4a	46	6.5	7.1
B4b	55	6	9.2
B7a	69	10.5	6.6
B7b	75	7	10.7
B10a	72	9.5	7.6
B10b	75	8	9.4

Table 8. Dimensions of the craters produced by explosions located at 1.0 m above ground level (a)

Test	Mean diameter (cm)	Central depth (cm)	D/H_2 ratio
C1a	34	4	8.5
C2a	52	4	13
C4a	43.5	4	10.9

Table 9. Dimensions of the craters produced by underground explosions (b)

Test	Mean diameter (cm)	Central depth (cm)	D/H_2 ratio
C1b(92)	215	40	5.4
C2b(90)	268	49	5.5
C4b(87)	304	83	3.7
C7b(96)	347	107	3.2
C10b(98)	393	127	3.1

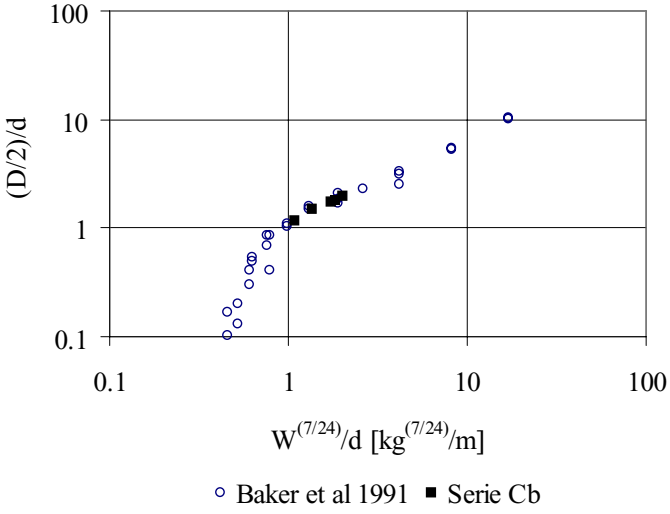

Fig. 9. Crater dimensions for underground explosions

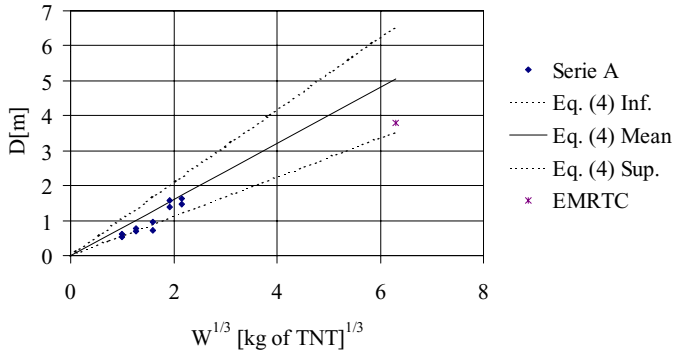

Fig. 10. Crater dimensions for explosions at ground level

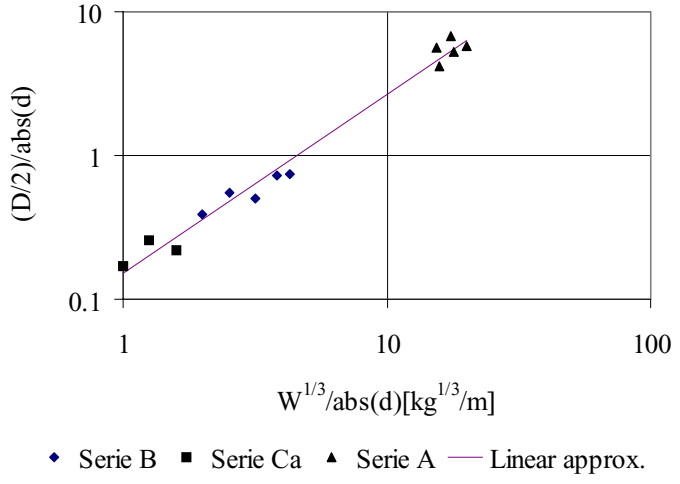

Fig. 11. Crater dimensions for explosions above ground level

line. This could be attributed to the fact that the charges were tangential to the surface and were not strictly on the ground surface. However, due to the small radius of the charges (0.05 m to 0.14 m for charges of 1 and 10 kg of TNT respectively) the results are appropriate. The result by EMRTC mentioned in Sect. 3 is also plotted in Fig. 10.

6.3 Explosions above ground level

In Fig. 11, the results from series B and Ca are presented (Tables 7 and 8). Moreover, the results corresponding to tangential explosions (Table 6) are incorporated considering the radius of the explosive as the height of the charges over the ground.

The dimensions of the crater for $d < 0$ (explosions above ground level) can be approximated by the following relationship:

$$\log\left(\frac{D/2}{|d|}\right) = 1.241 \log\left(\frac{W^{1/3}}{|d|}\right) - 0.818 \,. \qquad (5)$$

This expression can be useful in order to determine the mass of the explosive W from the diameter of the crater D and the height of the burst d.

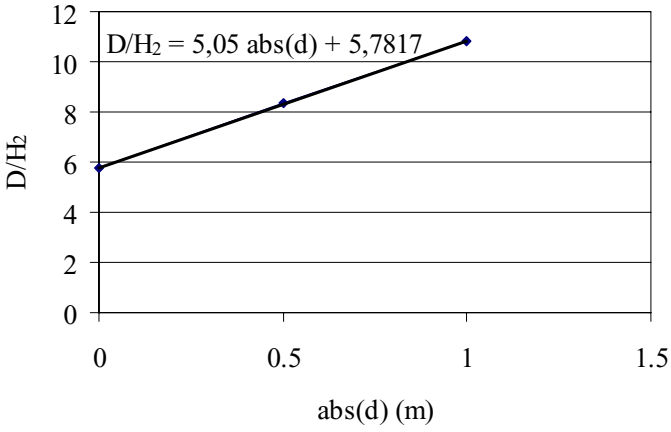

Fig. 12. Crater diameter/depth ratio for explosions above ground level

6.4 Relation diameter/depth

The statistical values of the diameter/depth ratios for the craters showed in Tables 6 to 9 are presented in Table 10. Underground explosions ($d > 0$) approximate the relation $D/H_2 = 4$ (Kinney and Graham 1985). The results for explosions on or above ground level are plotted in Fig. 12 as a function of the charge height d. It can be seen that a linear function provides an excellent description. The expression obtained is

$$D/H_2 = 5.78 + 5.05|d| \,. \qquad (6)$$

This expression can be useful in order to determine the height of the burst d from the diameter of the crater D and the depth of the crater H_2 at the centre of the crater. Obviously, the validity of Eq. (6) is restricted to heights of the bursts lower than 1.0 m, but the height of the charges from terrorist attacks with vehicle bombs is of that order.

7 Conclusions

- The crater dimensions for underground explosions coincide with those found in the literature. For the soil described in this paper (Tables 1 to 4) a relation can be found between the apparent crater diameter D, the mass of the explosive $W^{7/24}$ and the height of the charge d, as suggested by Baker et al. (1991).
- The crater dimensions for explosions at ground level qualitatively conform to Eq. (4) of Kinney and Graham (1985).
- In the case of explosives located at a height above ground level, the craters were significantly smaller than those produced by explosions at ground level or underground. This result is of practical interest, because the data found in the open literature about this topic is scarce, and also because this is generally the case, when the explosive is being transported in trucks or cars.
- Two new single prediction equations for the dimensions of the crater produced by explosions over the ground are presented in Eqs. (5) and (6). The first expression can

Table 10. Statistical values of the relations diameter/depth for the craters by explosions above ground level

D/H_2 ratio	Underground explosions	Ground level explosions	0.5 m explosions	1.0 m explosions
Mean	4.18	5.75	8.37	10.8
Standard deviation	1.18	1.07	1.31	2.25
Coefficient of variation (%)	28.3	18.6	15.6	20.8

be useful in order to determine the mass of the explosive W from the diameter of the crater D and the height of the burst d. The second equation can be useful to determine the height of the burst d from the diameter of the crater D and the depth of the crater H_2 at the centre of the crater.

Acknowledgements. The authors wishes to thank the collaboration of Eng. Ruiz Martinez, the owner of the test field and Eng. Orlando, the explosives expert. Moreover, the financial support of the CONICET (Argentina) and CNPq (Brazil) is gratefully acknowledged. Special acknowledgements are extended to the reviewers of the first version of the paper, since their useful suggestions lead to many improvements of the final version.

References

Baker WE, Cox PA, Westine PS, Kulesz JJ, Strehlow RA (1983) Explosion hazards and evaluation. Elsevier, Amsterdam

Baker WE, Westine PS, Dodge FT (1991) Similarity methods in engineering dynamics. Elsevier, Amsterdam

Bull JW, Woodford CH (1998). Camouflets and their effects on runway supports. Computer and Structures 69/6: 695–706

Formby SA, Wharton RK (1996) Blast characteristics and TNT equivalence values for some commercial explosives detonated at ground level. Journal of Hazardous Materials 50: 183–198

Gorodilov LV, Sukhotin AP (1996) Experimental investigation of craters generated by explosions of underwater surface charges on sand. Combustion, Explosion, and Shock Waves, Vol. 32, No 3, 344–346

Iturrioz I, Riera JD (2001) Numerical Study of the Effect of Explosives On a Plane Surface, XII Congress on Numerical Methods and their Applications, ENIEF 2001, Córdoba, Argentina, In Spanish

Jones GHS, Roddy DJ, Henny RW, Slater JE (1997) Defence Research Establishment Suffield Explosion Craters and Planetary Impact Craters: Morphological and Structural Deformation Analogues, 15th International Symposium on Military Aspect of Blast and Shock, Alberta, Canada

Kinney GF, Graham KJ (1985) Explosive shocks in air. 2nd Edition, Springer Verlag, Berlin

Persson PA, Holmberg R., Lee J (1994) Rock blasting and explosives engineering, CRC Press, USA

Smith PD, Hetherington JG (1994) Blast and Ballistic Loading of Structures, Butterworth-Heinemann Ltd, Great Britain